MEDICAL SCIENCE MONITOR

ANIMAL STUDY

e-ISSN 1643-3750
© Med Sci Monit, 2021; 27: e930042
DOI: 10.12659/MSM.930042

Received: 2020.11.23
Accepted: 2021.01.18
Available online: 2021.03.08
Published: 2021.06.01

Post-Treatment Sevoflurane Protects Against Hypoxic-Ischemic Brain Injury in Neonatal Rats by Downregulating Histone Methyltransferase G9a and Upregulating Nuclear Factor Erythroid 2-Related Factor 2 (NRF2)

Authors' Contribution:
Study Design A
Data Collection B
Statistical Analysis C
Data Interpretation D
Manuscript Preparation E
Literature Search F
Funds Collection G

A 1 HuaiMing Wang
B 1 YiQuan Xu
E 1 Shuying Zhu
F 2 XueMing Li
G 1 HongWei Zhang

1 Department of Anesthesiology, Sichuan Cancer Hospital and Institute, Sichuan Cancer Center, School of Medicine, University of Electronic Science and Technology of China, Chengdu, Sichuan, P.R. China
2 Department of Radiology, Sichuan Cancer Hospital and Institute, Sichuan Cancer Center, School of Medicine, University of Electronic Science and Technology of China, Chengdu Sichuan,P.R. China

Corresponding Author: HongWei Zhang, e-mail: zhanghw0729@163.com
Source of support: This work was supported by the Health and Family Planning Commission of Sichuan Province (No. 17PJ217)

Background: Perinatal hypoxia and subsequent reduction of cerebral blood flow leads to neonatal hypoxic-ischemic brain injury (HIBI), resulting in severe disability and even death. Preconditioning or post-conditioning with sevoflurane protects against cerebral injury. This study investigated the mechanism of sevoflurane in HIBI.

Material/Methods: The HIBI model of neonatal rats was established and the model rats were post-treated with sevoflurane. The oxygen-glucose deprivation (OGD) cell model was established, and the OGD cells were transfected with NRF2-siRNA plasmid and post-treated with sevoflurane. The Morris water maze test was used to detect the motor activity, spatial learning, and memory ability of HIBI rats. Histological stainings were performed to observe the area of cerebral infarction, record the number of neurons in the hippocampus, and assess neuron apoptosis. The levels of inflammatory factors were detected by ELISA. The protein levels of histone methyltransferase G9a and histone H3 lysine 9 (H3K9me2) were detected by western blot assay. The apoptosis was detected by flow cytometry.

Results: Sevoflurane post-treatment significantly shortened the escape latency of HIBI neonatal rats, increased the density of neurons, reduced the area of cerebral infarction, and decreased the levels of inflammatory factors and neuronal apoptosis. Sevoflurane post-treatment decreased G9a and H3K9me2 levels, and G9a level was negatively correlated with NRF2 level. NRF2 silencing reversed the alleviation of sevoflurane post-treatment on OGD-induced cell injury.

Conclusions: Sevoflurane post-treatment promotes NRF2 expression by inhibiting G9a and H3K9me2, thus alleviating HIBI in neonatal rats.

Keywords: Animals, Newborn • Histone-Lysine N-Methyltransferase • Hypoxia-Ischemia, Brain

Full-text PDF: https://www.medscimonit.com/abstract/index/idArt/930042

3902 5 5 35

Indexed in: [Current Contents/Clinical Medicine] [SCI Expanded] [ISI Alerting System] [ISI Journals Master List] [Index Medicus/MEDLINE] [EMBASE/Excerpta Medica] [Chemical Abstracts/CAS]

Background

Hypoxic-ischemic brain injury (HIBI) is mainly characterized by a reduction in levels of blood flow and oxygen concentration, which results in an inefficient supply of nutrient substances to the brain [1]. HIBI is caused by birth asphyxia in neonates and cardiac arrest in infants or children, which is related to altered degrees of neurologic sequelae based upon the severity and length of HI [2]. Currently, therapeutic hypothermia for neuroprotection has made great advances, but the improvements remain modest in long-term neurological outcomes [3]. Approximately half of the survivors from HIBI suffer from immediate or delayed onset of neuropsychological sequelae, while a quarter of the survivors present major neurological impairments [4]. Therefore, it is vital to determine the mechanisms underlying brain injury and to seek effective therapeutic regimens for neonatal HIBI.

Numerous studies have explored the effects of different drugs and therapeutic strategies on HIBI neonatal rats together with the underlying mechanisms [5, 6]. Application of volatile anesthetics, such as sevoflurane and isoflurane, provides neuroprotection in HIBI in neonatal rats [7]. Sevoflurane is the most commonly used anesthetic in clinical practice because of its non-flavor and small blood gas distribution coefficient, which can induce anesthesia quickly [8]. Sevoflurane exerts a protective function in neuronal HIBI through suppressing apoptosis and necrosis [9]. However, the precise mechanisms of sevoflurane in neonatal HIBI remain to be determined.

Epigenetic mechanisms (eg, post-translational histone modification, DNA methylation, and small noncoding RNAs) play vital roles in human neurodegenerative diseases [10]. The histone methyltransferase G9a is considered to be a repressive mark by catalyzing the demethylation of lysine 9 of histone H3 (H3K9me2) [11, 12]. Recent reports have associated G9a with neuronal functions, including neurite growth, synaptic plasticity, neurogenesis, and neurodegeneration [13-16]. A study indicated that G9a-mediated elevation of H3K9me2 is implicated in the apoptosis and cognitive impairment caused by sevoflurane in the developing brain [17]. Nevertheless, the contribution of G9a to early neuronal development is unstudied. More importantly, Jiang et al found that BIX-01294 treatment or siRNA-mediated G9a knockdown contributes to the upregulation of nuclear factor erythroid 2-related factor 2 (NRF2) [18]. NRF2 is a redox-sensitive transcription factor that is responsible for the antioxidant defense system by regulating the expressions of various oxidant stress-related enzymes [19]. Promoting NRF2 antioxidant pathway suppresses NLRP3 inflammasome activation, thereby alleviating early brain injury after experimental intracerebral hemorrhage [20]. Enhanced NRF2 expression contributes to alleviating oxidative stress and inflammatory response in ischemia/reperfusion rats [21]. Lycopene exerts a neuroprotective effect on HI brain injury in neonatal rats via the NRF2/NF-κ pathway [22]. Currently, there has been little research on whether sevoflurane post-treatment regulates NRF2 via G9a to affect the HIBI in neonatal rats. The purpose of this study was to assess this issue, and to provide a new theoretical basis for the treatment of HIBI.

Material and Methods

Animal Model Establishment

Referring to the methods used in the literature [23], 7-day-old neonatal rats (Beijing Union-Genius Pharmaceutical Technology, Ltd, license number SYXK [Beijing] 2020-0021) were anesthetized by intraperitoneal injection of 3.5% pentobarbital sodium (50 mg/kg). The left common carotid artery was gently separated from the surrounding tissues at the median anterior cervical orifice and permanently ligated with 7-0 surgical silk thread, and then the incision was sutured. All operations were performed under sterile conditions within 5 min. The revived neonatal rats were placed in a cage together with the mother rats for 2 h, and then placed in a humidified environment with continuous input of 8% O_2 and 92% N_2 at 37°C for 2 h, and the oxygen concentration was continuously monitored. After that, the neonatal rats with HI induction were returned to the cage together with the mother rats.

Animal Treatment and Grouping

The 7-day-old neonatal rats were allocated into sham group (only the left neck was exposed without ligation nor hypoxia treatment), HI group, and sevoflurane post-treatment group (HI+S group, neonatal rats immediately inhaled 2% sevoflurane delivered by 30% O_2 and 70% N_2 humidified mixed gas for 30 min after induction of HI), with 18 rats in each group. The rats were euthanized 35 days after HI induction, among which 6 rats in each group were used for tetrazolium chloride (TTC) staining, 6 rats were used for Nissl staining and transferase-mediated deoxyuridine triphosphate-biotin nick-end labeling (TUNEL) staining, and 6 rats were used for detection of the protein extracted from homogenate.

An In Vitro Model of Oxygen-Glucose Deprivation (OGD)

PC12 cells (American Type Culture Collection, Manassas, USA) were cultured in Dulbecco's modified Eagle's medium (DMEM) at 37°C with 5% CO_2, which was supplemented with 10% (v/v) fetal bovine serum (FBS) and 1% (v/v) penicillin-streptomycin solution (complete growth medium). The medium was renewed every 3 days. Cells at passage 7-10 were cultured with glucose-free medium (pure DMEM without FBS or penicillin-streptomycin solution) in a hypoxic chamber with 1%

Indexed in: [Current Contents/Clinical Medicine] [SCI Expanded] [ISI Alerting System] [ISI Journals Master List] [Index Medicus/MEDLINE] [EMBASE/Excerpta Medica] [Chemical Abstracts/CAS]

oxygen for 3 h. Then, the complete growth medium was added and the cells were allowed to recover for 24 h to construct an OGD cell model.

Cell Treatment and Grouping

The plasmids needed for the experiment were constructed by Sangon Biotech (Shanghai). OGD-induced PC12 cells were transfected with overexpressed (oe)-negative control (NC), oe-G9a, NC-siRNA, and NRF2-siRNA as per the instructions of Lipofectamine 3000 (Thermo Fisher Scientific, Waltham, MA, USA) (plasmid/transfection reagent=1 μg/2.4 μL, siRNA/transfection reagent=12.5 pmoles/μL). After 24-h transfection at 37°C, cells were used for subsequent experiments.

Cells were assigned into blank group (PC12 cells without any treatment), OGD group, an OGD+S group (OGD-induced PC12 cells were cultured with 2% sevoflurane for 30 min), OGD+S+oe-NC group (OGD-induced PC12 cells transfected with overexpressed G9a control empty vector were cultured with 2% sevoflurane for 30 min), OGD+S+oe-G9a group (OGD-induced PC12 cells transfected with overexpressed G9a vector were cultured with 2% sevoflurane for 30 min), OGD+S+NC-siRNA group (OGD-induced PC12 cells transfected with silenced NRF2 control empty vector were cultured with 2% sevoflurane for 30 min), or OGD+S+NRF2-siRNA group (OGD-induced PC12 cells transfected with silenced NRF2 vector were cultured with 2% sevoflurane for 30 min).

Morris Water Maze (MWM) Test

The MWM test was performed on days 29 to 34 after HI (n=18 rats/group). The water maze was a black-walled circular swimming pool (diameter: 160 cm, depth: 60 cm), which was evenly divided into 4 quadrants. In the fourth quadrant, an escape platform (diameter: 12 cm) was hidden at a distance of 30 cm from the edge of the pool wall, and it was located about 1.5 cm below the water surface. The water temperature was controlled at (20±1) , and an automatic monitoring system was installed above the pool to synchronously record the movement of rats in the pool. One day before the experiment, the rats of each group were put into the pool (not including the platform) to swim freely for 90 s to make them familiar with the pool environment. The place navigation test was conducted every day at 8: 00, for a total of 5 days. Facing the wall of the pool, the rats were put into the water from the entry points of the 4 quadrants in random order, and they were forced to search for the underwater platform. The image monitoring system automatically tracked and recorded the total distance from entering the water to climbing onto the platform and the time required to climb onto the platform, that is, the escape latency. If a rat found the platform by itself within 90 s, it was allowed to stay on the platform for 20 s before the next rat was tested in the maze. If the platform could not be found within 90 s after entering the water, the rat was guided to the platform and allowed to stay for 20 s. At this time, the escape latency was determined to be 90 s. The rats were assessed 4 times a day, with an interval of at least 30 min each time, and the average value of the 4 escape latencies was calculated. After each experiment, the rats were wiped dry and put back into the cage to warm up and they had free access to food and water. After each training day, the water maze was cleaned and replaced with new water to eliminate the interference of smell and environmental factors. One day after the place navigation test, the platform was removed from the maze for the spatial probe test. The rats were placed at the water entry point in the second quadrant, and the number of times the rat swam through the platform area within 90 s was recorded as the number of times it crossed the platform.

TTC Staining

The rat brain tissues were placed in phosphate-buffered saline (PBS) solution at 4°C, frozen at -20°C for 30 min, and sliced into 2-mm sections. The sections were placed in 10 g/L TTC solution (Sinopharm Chemical Reagent Co., Ltd., Shanghai, China) in the dark at 37°C for 10 min, fixed overnight in 4% paraformaldehyde (Sigma-Aldrich, St. Louis, MO, USA), and observed under a microscope. The normal brain tissues were stained red, and the infarct tissues were stained white. Images were collected layer-by-layer, and the infarct area of each layer was calculated using Image J 1.43 software (National Institutes of Health, Bethesda, Maryland, USA).

Nissl Staining

The rat brain tissues were fixed in 4% malondialdehyde solution at room temperature for 24 h, embedded in paraffin, dehydrated with conventional ethanol, and made into 5-μm sections. The sections were stained with cresyl violet for 1 h, washed with 0.1 M PBS, and differentiated with Nissl differentiation solution under the microscope until the background was clear. The sections were then dehydrated in a graded alcohol solution and covered with a cover sheet with neutral resin. Image J 1.43 software (National Institutes of Health) was used to count the number of healthy and Nissl-positive neurons located in the hippocampus (n=10 rats/group) by investigators who were blinded to the experimental intervention. The density of Nissl-stained neurons was the ratio of the left and right hemispheres.

Enzyme-Linked Immunosorbent Assay (ELISA)

The rat brain tissues were thoroughly and evenly mixed with PBS in an ice bath, resuspended in the lysis buffer in the kit, centrifuged at 1500×g at 4°C for 15 min to obtain the

Indexed in: [Current Contents/Clinical Medicine] [SCI Expanded] [ISI Alerting System] [ISI Journals Master List] [Index Medicus/MEDLINE] [EMBASE/Excerpta Medica] [Chemical Abstracts/CAS]

supernatant, and further stored at -70°C. The levels of 4 inflammatory cytokines – tumor necrosis factor (TNF)-α, interleukin (IL)-1β, IL-6, and IL-8 were assessed according to the instructions of ELISA kits (Cloud-Clone Corp, Wuhan, China), and the absorbance value at 450 nm was measured on a microplate reader (RT-6100, Rayto, Shenzhen, China).

TUNEL Staining

The rat brain tissues (5 μm) were collected for TUNEL detection of cell apoptosis with the Apoptosis Detection Kit (ZK8005, Beijing Zhongshan GoldenBridge Biotechnology Co., Ltd., Beijing, China). An optical microscope (400×, BX50/Olympus, Japan) was used for observation in 5 randomly-selected areas. TUNEL staining was performed by an experimenter who did not know the grouping, and the apoptotic index (AI) was calculated as (the number of positive apoptotic cells/total number of cells)×100%.

Western Blot Assay

The brain tissue sections were deparaffinized with xylene, rehydrated with gradient ethanol in descending order, incubated with normal goat serum (Beyotime Institute of Biotechnology, Shanghai, China) for 20 min at room temperature, and then incubated with anti-G9A (1: 1000, ab185050, Abcam, Cambridge, USA), anti-Histone H3 (di methyl K9, 3 μg/mL, ab1220, Abcam), or anti-Nrf2 (1: 1000, ab137550, Abcam) overnight at 4°C. Subsequently, the sections were washed with PBS, then incubated with goat anti-rabbit IgG (1: 2000, ab205718, Abcam) at 37°C for 15 min, stained with 3,3'-diaminobenzidine, and counterstained with hematoxylin at 37°C for 3 min. Lastly, the sections were dehydrated in ethanol solution and cleaned with xylene. The protein level was observed with an optical microscope (Olympus), with β-actin as the internal control (1 μg/mL, ab8226, Abcam).

Flow Cytometry

Cells of each group were harvested and then centrifuged to remove the supernatant. Next, the cells were suspended in 1 mL 1×binding buffer, and centrifuged at 300×g for 10 min to remove the supernatant. Afterwards, the cells were resuspended with 1 mL 1×binding buffer to achieve a cell density of 1×10^6 cells/mL. Each tube was supplemented with 100 μL cells. Then, the tube was incubated with 5 μL Annexin V-fluorescein isothiocyanate and 5 μL propidium iodide at room temperature without light exposure for 5 min, followed by supplementation with PBS to 500 μL, and gentle blending. The cell apoptosis rate was calculated as (number of early apoptotic cells+number of late apoptotic cells)/number of non-apoptotic cells and was detected using a flow cytometer (MoFloAstrios EQ, Beckman Coulter, Inc, Fullerton, CA, USA) within 1 h.

Statistical Analysis

All data were analyzed and graphed using SPSS 22.0 statistical software (IBM Corp., Armonk, NY, USA) and Graph Prism 8.0, and the measurement data were expressed in the form of mean±standard deviation. First, tests for normality and homogeneity of variance were performed, and the data were determined to conform to normal distribution and homogeneity of variance. The comparison among multiple groups was conducted by one-way analysis of variance (ANOVA), followed by Tukey's multiple comparisons test. *P* less than 0.05 indicated that the difference was statistically significant.

Results

Sevoflurane Post-Treatment Reduces Cerebral Infarct Size and Cognitive Impairment in HIBI Neonatal Rats

The MWM test was performed to test the learning and memory ability of neonatal rats in each group. The results of escape latency (**Figure 1A**) showed that in the first 5 days, the escape latency of rats in each group was decreased. Compared with the sham-operated rats, the HIBI rats presented prolonged escape latency (all $P<0.001$) and the rats in the HI+S group showed shorter escape latency than those in the HI group (all $P<0.001$). The results of the spatial probe test (**Figure 1B**) demonstrated that the sham-operated rats had the most platform crossing times, and the crossing times of the HI+S group were significantly higher than those of HI group ($P=0.039$). The cerebral infarct size in rats of each group was detected by TTC staining (**Figure 1C**). White infarcts were seen in HIBI rats or HIBI rats with sevoflurane post-treatment, mainly located in the frontal, parietal, and temporal cortex. The infarct size in HIBI rats was larger compared in the sham-operated rats ($P<0.001$), while the infarct size in HIBI rats was decreased after sevoflurane post-treatment ($P<0.001$). The results suggested that ischemia and hypoxia caused long-term damage to learning and memory, and sevoflurane post-treatment alleviated the damage caused by ischemia and hypoxia (**Supplementary Table 1**).

Sevoflurane Post-Treatment Relieves Inflammation and Nerve Cell Apoptosis in HIBI Neonatal Rats

To explore the effect of sevoflurane post-treatment on brain tissues of HIBI rats, we performed Nissl staining to observe the positive nerve cells in the hippocampus of rats in each group. The results (**Figure 2A**) showed that the neonatal rats with HIBI presented reduced neuronal density ratio compared with the sham-operated rats ($P<0.001$), and sevoflurane post-treatment diminished the degree of decrease of neuronal density ratio induced by ischemia and hypoxia ($P<0.001$). Next, ELISA was used to measure the levels of inflammatory factors (TNF-α,

Indexed in: [Current Contents/Clinical Medicine] [SCI Expanded] [ISI Alerting System] [ISI Journals Master List] [Index Medicus/MEDLINE] [EMBASE/Excerpta Medica] [Chemical Abstracts/CAS]

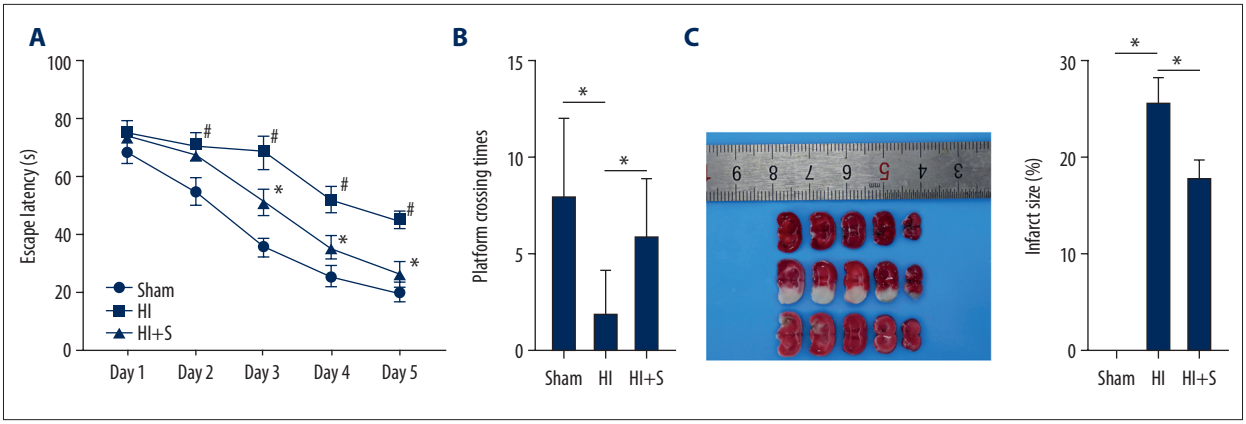

Figure 1. Sevoflurane post-treatment attenuates cognitive impairment in HIBI neonatal rats. (**A**) Escape latency of rats in each group assessed by Morris water maze test, N=18, # $P<0.001$, Sham group vs HI group; * $P<0.001$, HI group vs HI+S group. (**B**) The platform crossing times of rats in each group measured by spatial probe test, N=18. (**C**) The cerebral infarct size in rats of each group measured by TTC staining, N=6. The data are expressed as the mean±standard deviation. The data between groups were analyzed by one-way ANOVA, followed by Tukey's multiple comparisons test. * $P<0.05$.

IL-1β, IL-6, and IL-8) (**Figure 2B**, all $P<0.001$), and TUNEL staining was carried out to observe nerve cell apoptosis in brain tissues of HIBI neonatal rats (**Figure 2C**). The findings suggested that the levels of inflammatory factors and AI were higher in HIBI neonatal rats compared with the sham-operated rats ($P<0.001$), and the rats in the HI+S group showed lower levels of inflammatory factors and AI compared with those in the HI group ($P<0.001$). Our results suggested that that sevoflurane post-treatment alleviated the brain damage of HIBI neonatal rats by reducing the inflammation and nerve cell apoptosis (**Supplementary Table 2**).

Sevoflurane Post-Treatment Down-Regulates Histone Methyltransferase G9a Level

Previous research has shown that pharmacological inhibition of G9a can have a significant protective effect on mouse nerve cells, and G9a can increase H3K9me2 level in cells [24]. Hence, we speculated that sevoflurane post-treatment can regulate the G9a level to affect the H3K9me2 level. The protein levels of G9a and H3K9me2 in rat brain tissues of each group were detected by western blot analysis, and the protein levels of G9a and H3K9me2 were elevated in HIBI neonatal rats and were reduced upon sevoflurane post-treatment (**Figure 3**, all $P<0.001$), indicating that the sevoflurane post-treatment inhibited G9a and H3K9me2 levels in brain tissues of HIBI neonatal rats (**Supplementary Table 3**).

Sevoflurane Reduces OGD-Induced Cell Damage by Downregulating G9a and H3k9me2 Levels

To further explore the mechanisms by which sevoflurane mediated H3K9me2 level by reducing G9a level, we established an OGD cell model in vitro and transfected the G9a overexpression vector into OGD-induced PC12 cells after sevoflurane treatment, and then detected the protein levels of G9a and H3K9me2 in each group. We found that H3K9me2 level was positively correlated with G9a level (**Figure 4A**, $P<0.05$). ELISA indicated that overexpression of G9a reversed the inhibitory effect of sevoflurane on the inflammation in OGD-induced PC12 cells (**Figure 4B**, $P<0.001$). Similarly, the results of flow cytometry showed that the apoptotic rate in OGD-induced PC12 cells was increased after overexpression of G9a (**Figure 4C**, $P<0.001$). These data suggest that sevoflurane post-treatment reduced the levels of G9a and H3K9me2 in OGD-induced PC12 cells, further alleviating OGD-induced cell damage. After overexpression of G9a, the improvement effect of sevoflurane on OGD-induced cell damage was reversed (**Supplementary Table 4**).

Sevoflurane Reduces H3k9me2 Level and Promotes NRF2 Level to Relieve OGD-Induced Cell Damage

It is reported that G9a expression has a regulatory effect on NRF2 expression [18]. To further explore whether sevoflurane post-treatment promotes NRF2 level by inhibiting G9a and H3K9me2 level to alleviate the brain damage in HIBI neonatal rats, we used siRNA to silence NRF2 expression, with NC-siRNA as a control. Western blot analysis suggested that the NRF2 protein level was lower in the OGD+S+NRF2-siRNA group relative to that in the OGD+S group (**Figure 5A**, $P<0.001$). ELISA and flow cytometry were used to assess cell inflammatory factor levels and apoptosis. We found that there was an elevation in the inflammatory factor levels and apoptosis rate of cells in the OGD+S+NRF2-siRNA group relative to that in the OGD+S group (**Figure 5B, 5C**, all $P<0.05$). Taken together, our results show that NRF2 silencing reversed the protective function of sevoflurane in alleviating the OGD-induced cell damage, indicating that sevoflurane increased the NRF2 level by

Indexed in: [Current Contents/Clinical Medicine] [SCI Expanded] [ISI Alerting System] [ISI Journals Master List] [Index Medicus/MEDLINE] [EMBASE/Excerpta Medica] [Chemical Abstracts/CAS]

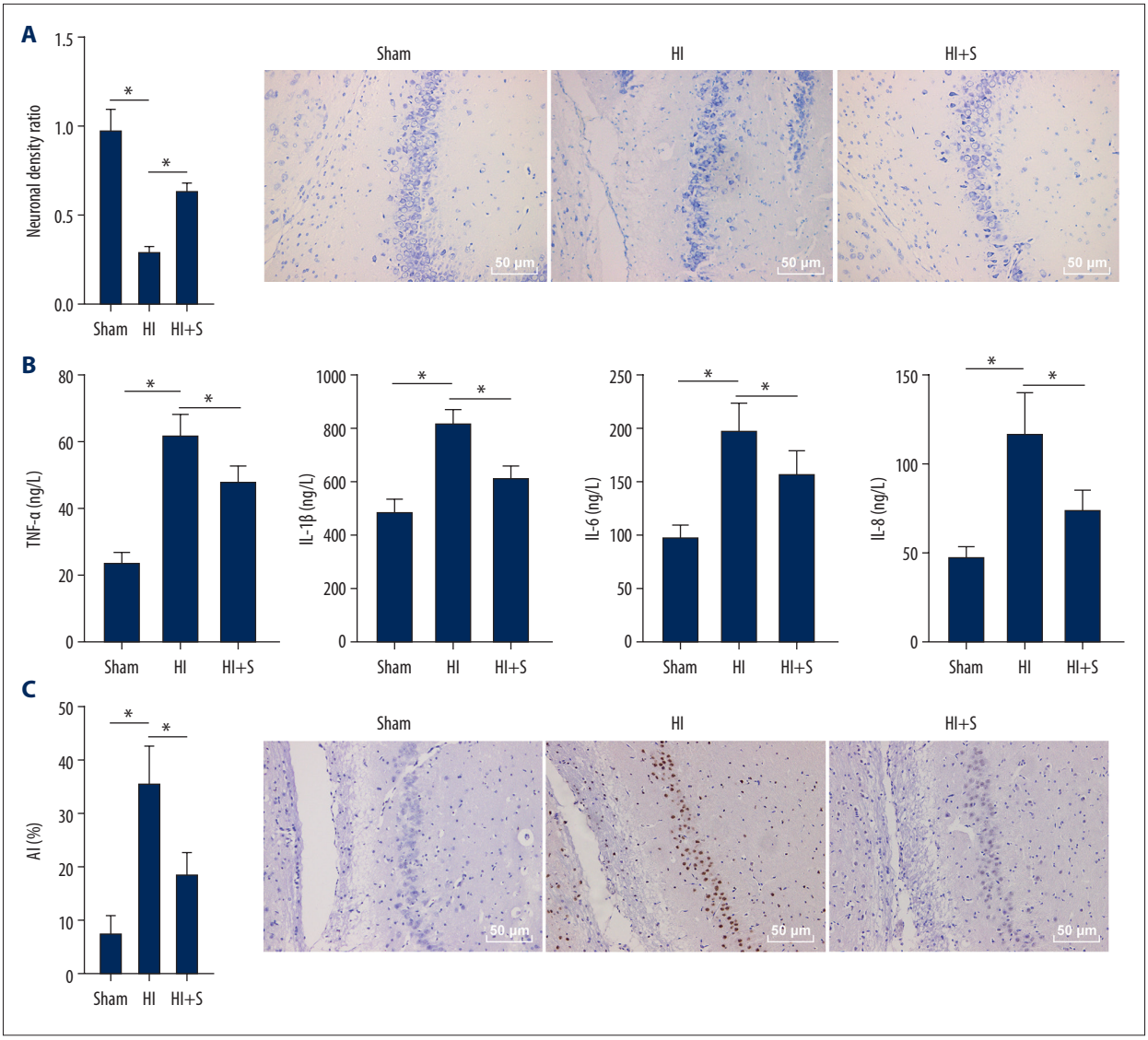

Figure 2. Sevoflurane post-treatment relieves inflammation and nerve cell apoptosis in HIBI neonatal rats. (**A**) Nissl staining was performed on the hippocampus of rat brain tissues in each group, and we compared the neuronal density ratios. (**B**) ELISA was used to measure the levels of inflammatory factors (TNF-α, IL-1β, IL-6, and IL-8) in rats of each group. (**C**) TUNEL staining was carried out to observe nerve cell apoptosis in brain tissues of rats in each group. N=6. The data are expressed as the mean±standard deviation. The data among groups were analyzed by one-way ANOVA, followed by Tukey's multiple comparisons test. * $P<0.05$.

reducing G9a and H3K9me2, thereby relieving HIBI in neonatal rats (**Supplementary Table 5**).

Discussion

HIBI in neonates can result in lifelong cognitive and memory impairments, which profoundly affect patients, families, and society [25]. However, no practical interventions are now available to treat neonatal brain injury in clinical practice, suggesting an urgency to identify interventions. In this study, we elucidated the mechanisms of sevoflurane in HIBI neonatal rats by establishing an in vivo rat model of HIBI and an in vitro model of OGD in PC12 cells. Collectively, our study suggests that post-treatment of sevoflurane attenuated HIBI in neonatal rats by inhibiting G9a and H3K9me2 levels.

Sevoflurane post-conditioning has been reported to strengthen cardiac resistance to ischemia-reperfusion injury in both experimental and clinical studies [26,27]. Recent research has demonstrated that post-conditioning using sevoflurane provided long-term neuroprotection to HIBI neonatal rats [23]. To

Indexed in: [Current Contents/Clinical Medicine] [SCI Expanded] [ISI Alerting System] [ISI Journals Master List] [Index Medicus/MEDLINE] [EMBASE/Excerpta Medica] [Chemical Abstracts/CAS]

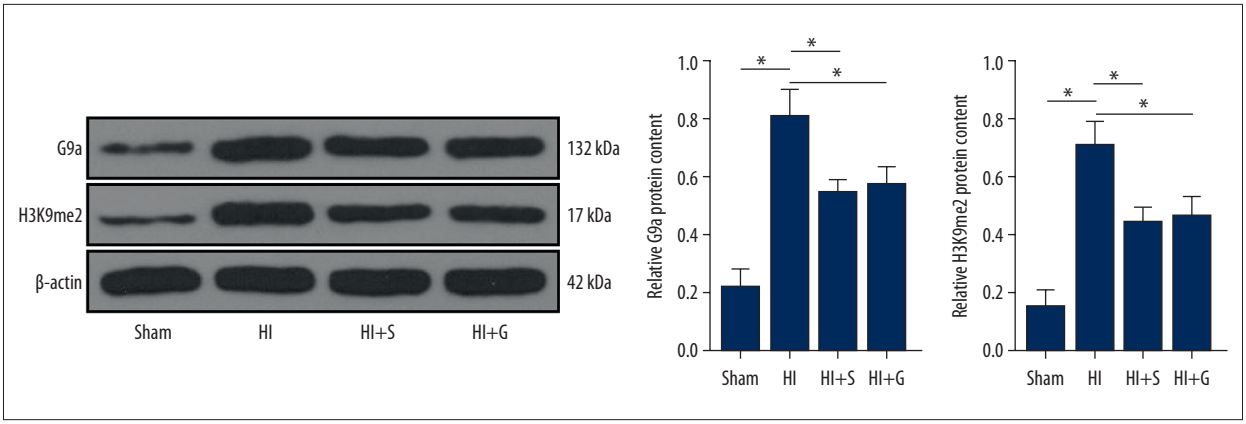

Figure 3. Sevoflurane post-treatment inhibits G9a and H3K9me2 expression in brain tissues of HIBI neonatal rats. The protein levels of G9a and H3K9me2 in rat brain tissues of each group were detected by western blot analysis. N=6. The data are expressed as the mean±standard deviation. The data among groups were analyzed by one-way ANOVA, followed by Tukey's multiple comparisons test. * $P<0.05$.

investigate the effect of sevoflurane post-treatment on HIBI, we performed a series of assays to assess motor activity, spatial learning, and memory ability of neonatal HIBI rats, as well as to observe the area of cerebral infarction, measure the levels of inflammatory factors, and assess neuron apoptosis. We found that sevoflurane post-treatment significantly shortened the escape latency of HIBI neonatal rats, increased the density of neurons, and reduced the area of cerebral infarction, the levels of inflammatory factors, and the apoptosis of neurons. The inflammatory factors IL-1, IL-6, and TNF-α have been revealed to be essential mediators of inflammatory response in cerebral ischemia, and sevoflurane post-treatment confers neuroprotection through anti-inflammatory effects [28]. Of note, a previous study found that neuroprotection with sevoflurane before brain ischemia may be mediated by restriction of brain inflammation [7]. All this evidence demonstrates the protective role of sevoflurane in HIBI.

Histone methyltransferase regulates the transcription level of downstream target genes by methylation modification of histone at different sites (such as H3K9me2 and H3K27me3) [29]. Our study showed that histone methyltransferase G9a increased the level of H3K9me2. More importantly, research has focused on the association between G9a and neurons [30]. Griñán-Ferré et al have also found that pharmacological inhibition of G9a can have a protective effect on mouse nerve cells [24]. We speculate that sevoflurane post-treatment affects the H3K9me2 level by regulating the G9a level. The findings of our study indicated that elevated levels of G9a and H3K9me2 were found in HIBI neonatal rats, which were reduced after sevoflurane post-treatment, indicating that sevoflurane post-treatment inhibited the levels of G9a and H3K9me2 in brain tissues of HIBI neonatal rats. To further explore the mechanism by which sevoflurane mediates the level of H3K9me2 by reducing G9a level, we established an OGD cell model in vitro. The findings indicated that sevoflurane post-treatment reduced the G9a and H3K9me2 levels in OGD-induced PC12 cells, further alleviating OGD-induced cell damage. G9a and G9a-like protein are primary enzymes for H3K9me2 that downregulate the expression of genes [11,12]. In addition, our results suggest that overexpression of G9a reversed the inhibitory effect of sevoflurane post-treatment on OGD-induced cell inflammation and reversed the improvement effect of sevoflurane post-treatment on OGD-induced cell damage. Schweizer et al found that inhibition of the histone methyltransferases G9a enhances neuronal survival after OGD [31]. It has also been demonstrated that G9a-mediated histone H3K9 and K27 demethylation modulates neurodegeneration in the developing brain [32]. In line with our findings, Yang et al reported that sevoflurane exposure increases G9a activity and subsequently enhances H3K9me2 level in the hippocampus [17].

With the increase of H3K9me2, the binding of H3K9me2 with downstream gene promoter is decreased, which inhibits the transcription of the downstream gene [33]. G9a expression has been found to exert a regulatory effect on NRF2 expression [18]. Gupta et al stated that administration of G9a inhibitor attenuates the induction of H3K9me2 and then activates NRF2 to decrease oxidative stress [33]. Our study revealed that G9a increased H3K9me2 level, but decreased NRF2 level, which indicated that G9a inhibited the NRF2 level by increasing the H3K9me2 level. The next step was to further explore whether sevoflurane post-treatment promoted the NRF2 level by inhibiting G9a and H3K9me2 levels, thereby alleviating the heart and brain damage in HIBI neonatal rats. The obtained results indicated that sevoflurane increased the NRF2 level by downregulating G9a and H3K9me2, playing a protective role in HIBI neonatal rats. The application of delayed remote ischemic preconditioning produces an additive cardioprotection to sevoflurane post-conditioning through elevated

Indexed in: [Current Contents/Clinical Medicine] [SCI Expanded] [ISI Alerting System] [ISI Journals Master List] [Index Medicus/MEDLINE] [EMBASE/Excerpta Medica] [Chemical Abstracts/CAS]

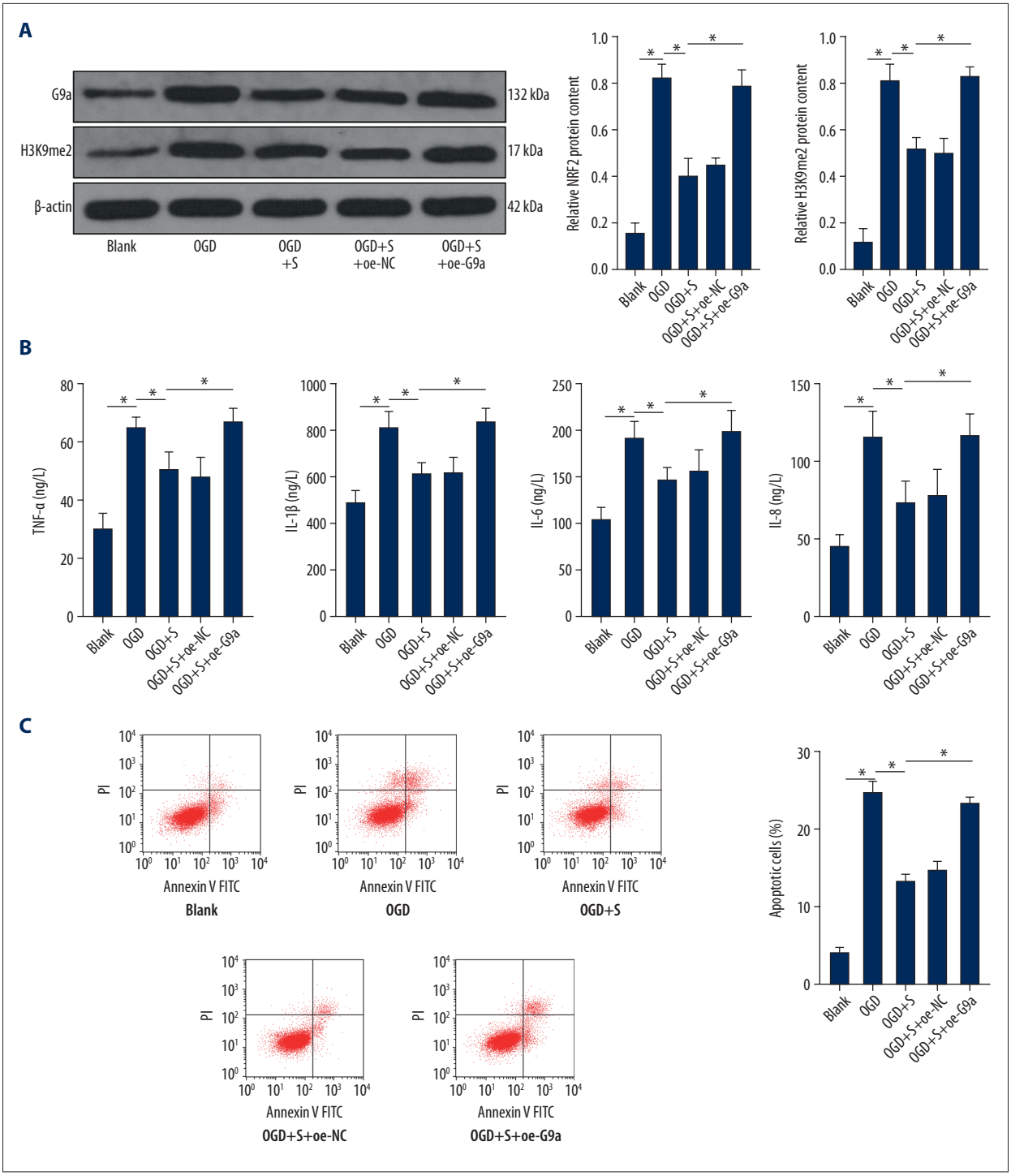

Figure 4. Sevoflurane post-treatment reduces the levels of G9a and H3K9me2 in OGD-induced PC12 cells to alleviate OGD-induced cell damage. (**A**) The protein levels of G9a and H3K9me2 in cells of each group were detected by western blot analysis. (**B**) ELISA was utilized to measure the levels of inflammatory factors (TNF-α, IL-1β, IL-6, and IL-8) in cells of each group. (**C**) Flow cytometry was performed to detect the apoptosis rate of cells in each group. The data are expressed as the mean±standard deviation. The data among groups were analyzed by one-way ANOVA, followed by Tukey's multiple comparisons test.
* $P<0.05$.

Indexed in: [Current Contents/Clinical Medicine] [SCI Expanded] [ISI Alerting System] [ISI Journals Master List] [Index Medicus/MEDLINE] [EMBASE/Excerpta Medica] [Chemical Abstracts/CAS]

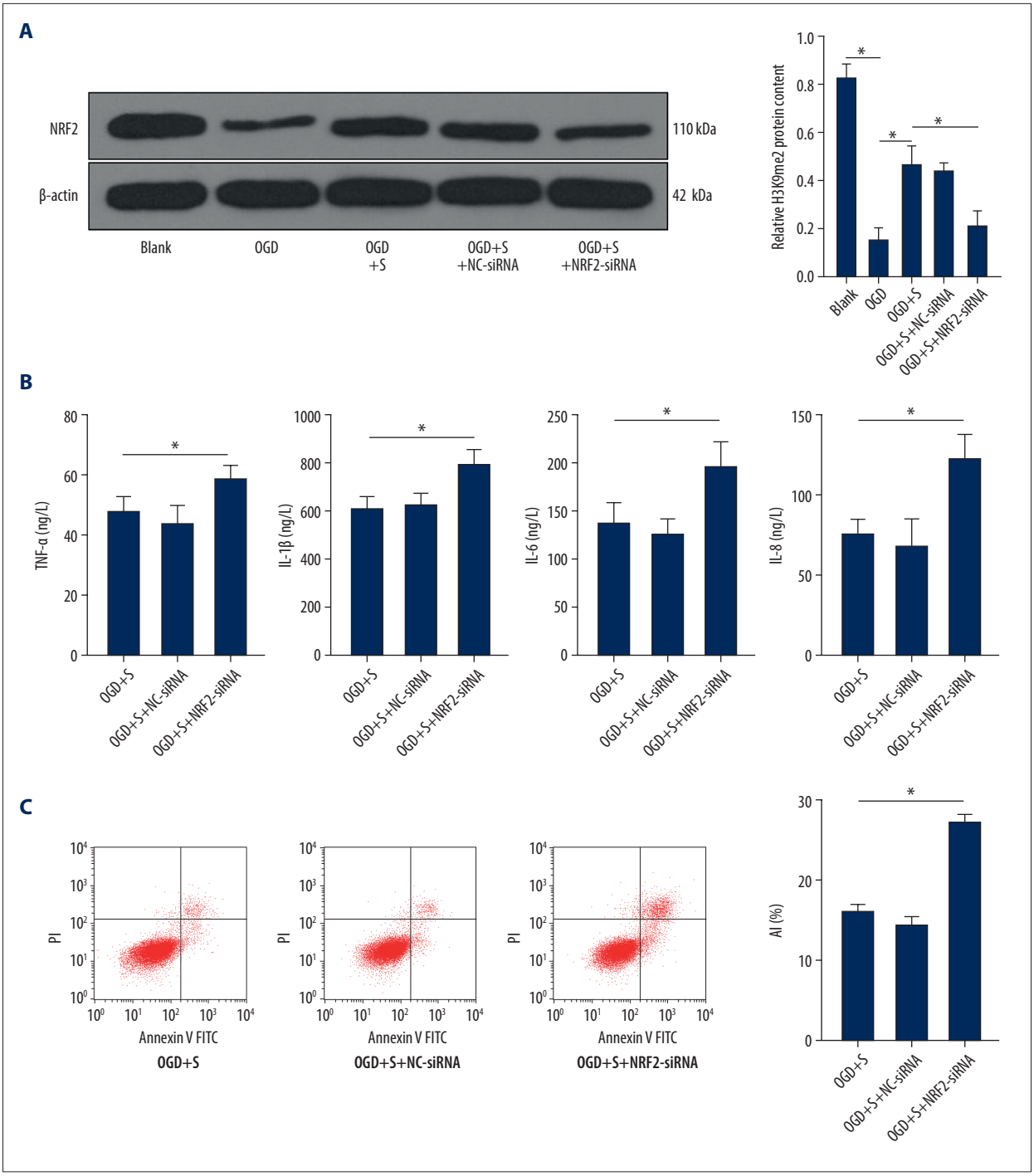

Figure 5. Silencing NRF2 reverses the alleviating effect of sevoflurane post-treatment on HIBI neonatal rats. (**A**) NRF2 protein level in cells of each group was determined by western blot assay. (**B**) ELISA was utilized to measure the levels of inflammatory factors (TNF-α, IL-1β, IL-6, and IL-8) in cells of each group. (**C**) Flow cytometry was carried out to observe apoptosis in cells of each group. The data are expressed as the mean±standard deviation. The data among groups were analyzed by one-way ANOVA, followed by Tukey's multiple comparisons test. * $P<0.05$.

Indexed in: [Current Contents/Clinical Medicine] [SCI Expanded] [ISI Alerting System] [ISI Journals Master List] [Index Medicus/MEDLINE] [EMBASE/Excerpta Medica] [Chemical Abstracts/CAS]

HO-1, partly via NRF2 translocation [34]. Another study has shown that NRF2 is involved in the neuroprotective effects of sevoflurane post-conditioning against oxidative damage at a specific time point [35]. However, the main genes and molecular mechanism involved in the neuroprotective effects of sevoflurane post-conditioning in HIBI remain to be determined.

Conclusions

In summary, our study suggests that sevoflurane post-treatment promotes NRF2 level by inhibiting G9a and H3K9me2, thus alleviating HIBI in neonatal rats. Our findings may provide valuable information on the underlying molecular mechanism of sevoflurane post-treatment, along with potential therapeutic targets to overcome HIBI with the involvement of G9a/NRF2. However, the specific regulatory mechanisms of sevoflurane post-treatment on G9a and NRF2 level has not been studied in-depth, which needs further verification. Moreover, we shall conduct further in vitro studies in other cell lines or primary cultured cells from rats.

Availability of Data and Materials

All the data generated or analyzed during this study are included in this published article.

Confloict of Interests

None.

Supplementary Data

Supplementary Table 1. Post-treatment of sevoflurane attenuates cognitive impairment in HIBI neonatal rats.

A. The escape latency of rats in each group examined by Morris water maze test.

Escape latency (s)	Sham	HI	HI+S	F value	DF
Day1	68.1±3.5	74.8±2.1	74.1±4.8		
Day2	54.8±4.8	70.2±4.7*	67.7±2.4		
Day3	35.2±3.0	68.3±5.7*	51.0±4.6**	356.2	2
Day4	25.4±3.6	52.1±4.4*	35.1±3.9**		
Day5	19.7±3.4	44.8±3.1*	26.0±4.4**		

One-way ANOVA was used to compare the mean difference among the three groups. Tukey's multiple comparisons test was used for post hoc test. F value correspond to the treatment, the time and the interaction between treatment and time in the one-way ANOVA; * $p<0.001$ between sham group and HI group, ** $p<0.001$ between HI group and HI+S group.

B. The platform crossing times of rats in each group measured by spatial probe test.

	Sham	HI	HI+S	F value	DF
Platform crossing times	8.1±3.8	2.3±2.0*	5.9±3.1**	8.903	2

One-way ANOVA was used to compare the mean difference among the three groups. Tukey's multiple comparisons test was used for post hoc test. * $p<0.001$ between sham group and HI group, ** $p<0.05$ between HI group and HI+S group.

C. The cerebral infarct size of rats in each group measured by TTC staining.

	Sham	HI	HI+S	F value	DF
Infarct size (%)	0±0	26.1±2.4*	17.7±1.7**	369.4	2

One-way ANOVA was used to compare the mean difference among the three groups. Tukey's multiple comparisons test was used for post hoc test. * $p<0.001$ between sham group and HI group, ** $p<0.001$ between HI group and HI+S group.

Indexed in: [Current Contents/Clinical Medicine] [SCI Expanded] [ISI Alerting System] [ISI Journals Master List] [Index Medicus/MEDLINE] [EMBASE/Excerpta Medica] [Chemical Abstracts/CAS]

Supplementary Table 2. Sevoflurane post-treatment relieves inflammation and nerve cell apoptosis in HIBI neonatal rats.

A. The comparison of neuronal density ratio.

	Sham	HI	HI+S	F value	DF
Neuronal density ratio	1.00±0.05	0.30±0.03*	0.65±0.04**	441.0	2

One-way ANOVA was used to compare the mean difference among the three groups. Tukey's multiple comparisons test was used for post hoc test. * p<0.001 between sham group and HI group, ** p<0.001 between HI group and HI+S group.

B1. The TNF-α level of rats in each group measured by ELISA.

	Sham	HI	HI+S	F value	DF
TNF-α (ng/L)	24.1±2.8	62.4±5.9*	48.1±4.5**	107.2	2

One-way ANOVA was used to compare the mean difference among the three groups. Tukey's multiple comparisons test was used for post hoc test. * p<0.001 between sham group and HI group, ** p<0.001 between HI group and HI+S group.

B2. The IL-1β level of rats in each group measured by ELISA.

	Sham	HI	HI+S	F value	DF
IL-1β (ng/L)	0±0	26.1±2.4*	17.7±1.7**	369.4	2

One-way ANOVA was used to compare the mean difference among the three groups. Tukey's multiple comparisons test was used for post hoc test. * p<0.001 between sham group and HI group, ** p<0.001 between HI group and HI+S group.

B3. IL-6 level of rats in each group measured by ELISA.

	Sham	HI	HI+S	F value	DF
IL-6 (ng/L)	101.1±9.5	201.4±24.7*	158.7±20.1**	41.29	2

One-way ANOVA was used to compare the mean difference among the three groups. Tukey's multiple comparisons test was used for post hoc test. * p<0.001 between sham group and HI group, ** p<0.05 between HI group and HI+S group.

B4. IL-8 level of rats in each group measured by ELISA.

	Sham	HI	HI+S	F value	DF
IL-8 (ng/L)	249.1±4.8	117.9±21.1*	74.7±10.0**	38.30	2

One-way ANOVA was used to compare the mean difference among the three groups. Tukey's multiple comparisons test was used for post hoc test. * p<0.001 between sham group and HI group, ** p<0.001 between HI group and HI+S group.

C. Nerve cell apoptosis in brain tissues of rats in each group measured by TUNEL staining.

	Sham	HI	HI+S	F value	DF
AI (%)	8.4±2.8	36.1±6.8*	18.6±4.3**	48.68	2

One-way ANOVA was used to compare the mean difference among the three groups. Tukey's multiple comparisons test was used for post hoc test. * p<0.001 between sham group and HI group, ** p<0.001 between HI group and HI+S group.

Indexed in: [Current Contents/Clinical Medicine] [SCI Expanded] [ISI Alerting System] [ISI Journals Master List] [Index Medicus/MEDLINE] [EMBASE/Excerpta Medica] [Chemical Abstracts/CAS]

Supplementary Table 3. Sevoflurane post-treatment relieves inflammation and nerve cell apoptosis in HIBI neonatal rats.

A. The G9a level of rat brain tissues in each group detected by western blot analysis.

	Sham	HI	HI+S	F value	DF
Relative G9a protein level	0.23±0.05	0.82±0.08*	0.56±0.03**	0.58 ± 0.05***	114.7

One-way ANOVA was used to compare the mean difference among the four groups. Tukey's multiple comparisons test was used for post hoc test. * $p<0.001$ between sham group and HI group, ** $p<0.001$ between HI group and HI+S group, *** $p<0.001$ between HI group and HI+G group.

B. The H3K9me2 level of rat brain tissues in each group detected by western blot analysis.

	Sham	HI	HI+S	F value	DF
Relative H3K9me2 protein level	0.16±0.05	0.72±0.07*	0.45±0.04**	0.47±0.06***	99.94

One-way ANOVA was used to compare the mean difference among the four groups. Tukey's multiple comparisons test was used for post hoc test. * $p<0.001$ between sham group and HI group, ** $p<0.001$ between HI group and HI+S group, *** $p<0.001$ between HI group and HI+G group.

Table 4. Sevoflurane post-treatment reduces the levels of G9a and H3K9me2 in OGD-induced PC12 cells to alleviate OGD-induced cell damage.

A1. G9a level of cells in each group detected by western blot analysis.

	Blank	OGD	OGD+S	OGD+S+oe-NC	OGD+S+oe-G9a	F value	DF
Relative G9a protein level	0.16±0.04	0.83±0.05*	0.41±0.07**	0.46±0.02	0.79±0.07***	82.29	4

One-way ANOVA was used to compare the mean difference among the five groups. Tukey's multiple comparisons test was used for post hoc test. * $p<0.001$ between blank group and OGD group, ** $p<0.001$ between OGD group and OGD+S group, *** $p<0.001$ between OGD+S group and OGD+S+oe-G9a group.

A2. H3K9me2 level of cells in each group detected by western blot analysis.

	Blank	OGD	OGD+S	OGD+S+oe-NC	OGD+S+oe-G9a	F value	DF
Relative H3K9me2 protein level	0.16±0.04	0.83±0.05*	0.41±0.07**	0.46±0.02	0.79±0.07***	88.24	4

One-way ANOVA was used to compare the mean difference among the five groups. Tukey's multiple comparisons test was used for post hoc test, * $p<0.001$ between blank group and OGD group, ** $p<0.001$ between OGD group and OGD+S group, *** $p<0.001$ between OGD+S group and OGD+S+oe-G9a group.

B1. TNF-α level of cells in each group measured by ELISA.

	Blank	OGD	OGD+S	OGD+S+oe-NC	OGD+S+oe-G9a	F value	DF
TNF-α (ng/L)	30.2±5.1	65.1±3.7*	51.1±5.3**	48.7±5.7	67.2±4.9***	26.81	4

One-way ANOVA was used to compare the mean difference among the five groups. Tukey's multiple comparisons test was used for post hoc test, * $p<0.001$ between blank group and OGD group, ** $p<0.05$ between OGD group and OGD+S group, *** $p<0.05$ between OGD+S group and OGD+S+oe-G9a group.

Indexed in: [Current Contents/Clinical Medicine] [SCI Expanded] [ISI Alerting System] [ISI Journals Master List] [Index Medicus/MEDLINE] [EMBASE/Excerpta Medica] [Chemical Abstracts/CAS]

B2. IL-1β level of cells in each group measured by ELISA.

	Blank	OGD	OGD+S	OGD+S+oe-NC	OGD+S+oe-G9a	F value	DF
IL-1β (ng/L)	501.2±40.8	826.4±56.1*	624.1±37.7**	630.7±51.3	851.2±47***	29.81	4

One-way ANOVA was used to compare the mean difference among the five groups. Tukey's multiple comparisons test was used for post hoc test, * $p<0.001$ between blank group and OGD group, ** $p<0.05$ between OGD group and OGD+S group, *** $p<0.05$ between OGD+S group and OGD+S+oe-G9a group.

B3. IL-6 level of cells in each group measured by ELISA.

	Blank	OGD	OGD+S	OGD+S+oe-NC	OGD+S+oe-G9a	F value	DF
IL-6 (ng/L)	105.6±11.1	194.2±16.4*	149.2±12.1**	157.9±21.4	202.1±20***	16.13	4

One-way ANOVA was used to compare the mean difference among the three groups. Tukey's multiple comparisons test was used for post hoc test, * $p<0.001$ between blank group and OGD group, ** $p<0.05$ between OGD group and OGD+S group, *** $p<0.05$ between OGD+S group and OGD+S+oe-G9a group.

B4. IL-8 level of cells in each group measured by ELISA.

	Blank	OGD	OGD+S	OGD+S+oe-NC	OGD+S+oe-G9a	F value	DF
IL-8 (ng/L)	47.2±5.8	116.7±15.2*	74.3±13.3**	79.2±16.9	117.9±13***	15.24	4

One-way ANOVA was used to compare the mean difference among the five groups. Tukey's multiple comparisons test was used for post hoc test, * $p<0.001$ between blank group and OGD group, ** $p<0.05$ between OGD group and OGD+S group, *** $p<0.05$ between OGD+S group and OGD+S+oe-G9a group.

C. apoptosis rate of cells in each group detected by flow cytometry.

	Blank	OGD	OGD+S	OGD+S+oe-NC	OGD+S+oe-G9a	F value	DF
Apoptotic cells (%)	4.29±0.31	24.91±1.25*	13.29±0.79**	14.82±0.92	23.59±0.47***	316.4	4

One-way ANOVA was used to compare the mean difference among the five groups. Tukey's multiple comparisons test was used for post hoc test, * $p<0.001$ between blank group and OGD group, ** $p<0.001$ between OGD group and OGD+S group, *** $p<0.001$ between OGD+S group and OGD+S+oe-G9a group.

Indexed in: [Current Contents/Clinical Medicine] [SCI Expanded] [ISI Alerting System] [ISI Journals Master List] [Index Medicus/MEDLINE] [EMBASE/Excerpta Medica] [Chemical Abstracts/CAS]

Table 5. Silencing NRF2 reverses the alleviating effect of sevoflurane post-treatment on HIBI neonatal rats.

A. NRF2 level of cells in each group determined by western blot assay.

	Blank	OGD	OGD+S	OGD+S+NC-siRNA	OGD+S+NRF2-siRNA	F value	DF
Neuronal density ratio	0.83±0.05	0.16±0.04*	0.47±0.07**	0.44±0.03	0.21±0.06***	78.52	4

One-way ANOVA was used to compare the mean difference among the five groups. Tukey's multiple comparisons test was used for post hoc test, * $p<0.001$ between blank group and OGD group, ** $p<0.001$ between OGD group and OGD+S group, *** $p<0.001$ between OGD+S group and OGD+S+NRF2-siRNA group.

B1. TNF-α level of cells in each group measured by ELISA.

	OGD+S	OGD+S+NC-siRNA	OGD+S+NRF2-siRNA	F value	DF
TNF-α (ng/L)	48.2±4.5	45.3±4.7	58.8±4.1*	7.684	2

One-way ANOVA was used to compare the mean difference among the three groups. Tukey's multiple comparisons test was used for post hoc test, * p<0.05 between OGD+S group and OGD+S+NRF2-siRNA group.

B2. IL-1β level of cells in each group measured by ELISA.

	OGD+S	OGD+S+NC-siRNA	OGD+S+NRF2-siRNA	F value	DF
IL-1β (ng/L)	620.2±39.2	630.7±44.8	806±50.1*	15.87	2

One-way ANOVA was used to compare the mean difference among the three groups. Tukey's multiple comparisons test was used for post hoc test, * $p<0.05$ between OGD+S group and OGD+S+NRF2-siRNA group.

B3. IL-6 level of cells in each group measured by ELISA.

	OGD+S	OGD+S+NC-siRNA	OGD+S+NRF2-siRNA	F value	DF
IL-6 (ng/L)	138.2±19.7	123.8±17.7	195.4±24*	10.11	2

One-way ANOVA was used to compare the mean difference among the three groups. Tukey's multiple comparisons test was used for post hoc test, * $p<0.05$ between OGD+S group and OGD+S+NRF2-siRNA group.

B4. IL-8 level of cells in each group measured by ELISA.

	OGD+S	OGD+S+NC-siRNA	OGD+S+NRF2-siRNA	F value	DF
IL-8 (ng/L)	75.3±10.3	69.8±15.5	124.1±15*	14.07	2

One-way ANOVA analysis was used to compare the mean difference among the three groups. Tukey's multiple comparisons test was used for post hoc test, * $p<0.05$ between OGD+S group and OGD+S+NRF2-siRNA group.

C. The apoptosis rate of cells in each group detected by flow cytometry.

	OGD+S	OGD+S+NC-siRNA	OGD+S+NRF2-siRNA	F value	DF
AI (%)	8.4±2.8	36.1±6.8	18.6±4.3*	48.68	2

One-way ANOVA was used to compare the mean difference among the three groups. Tukey's multiple comparisons test was used for post hoc test, * $p<0.001$ between OGD+S group and OGD+S+NRF2-siRNA group.

Indexed in: [Current Contents/Clinical Medicine] [SCI Expanded] [ISI Alerting System] [ISI Journals Master List] [Index Medicus/MEDLINE] [EMBASE/Excerpta Medica] [Chemical Abstracts/CAS]

References:

1. Toro-Urrego N, Vesga-Jimenez DJ, Herrera MI, et al. Neuroprotective role of hypothermia in hypoxic-ischemic brain injury: Combined therapies using estrogen. Curr Neuropharmacol. 2019;17(9):874-90
2. Bhalala US, Koehler RC, Kannan S. Neuroinflammation and neuroimmune dysregulation after acute hypoxic-ischemic injury of developing brain. Front Pediatr. 2014;2:144
3. Negro S, Benders M, Tataranno ML, et al. Early prediction of hypoxic-ischemic brain injury by a new panel of biomarkers in a population of term newborns. Oxid Med Cell Longev. 2018;2018:7608108
4. Fineschi V, Viola RV, La Russa R, et al. A controversial medicolegal issue: Timing the onset of perinatal hypoxic-ischemic brain injury. Mediators Inflamm. 2017;2017:6024959
5. Xu Y, Xue H, Zhao P, et al. Isoflurane postconditioning induces concentration- and timing-dependent neuroprotection partly mediated by the GluR2 AMPA receptor in neonatal rats after brain hypoxia-ischemia. J Anesth. 2016;30(3):427-36
6. Daadi MM, Davis AS, Arac A, et al. Human neural stem cell grafts modify microglial response and enhance axonal sprouting in neonatal hypoxic-ischemic brain injury. Stroke 2010;41(3):516-23
7. Ren X, Wang Z, Ma H, Zuo Z. Sevoflurane postconditioning provides neuroprotection against brain hypoxia-ischemia in neonatal rats. Neurol Sci. 2014;35(9):1401-4
8. Xue H, Xu Y, Wang S, et al. Sevoflurane post-conditioning alleviates neonatal rat hypoxic-ischemic cerebral injury via Ezh2-regulated autophagy. Drug Des Devel Ther. 2019;13:1691-706
9. Wang S, Xue H, Xu Y, et al. Sevoflurane postconditioning inhibits autophagy through activation of the extracellular signal-regulated kinase cascade, alleviating hypoxic-ischemic brain injury in neonatal rats. Neurochem Res. 2019;44(2):347-56
10. Coppede F. The potential of epigenetic therapies in neurodegenerative diseases. Front Genet. 2014;5:220
11. Shinkai Y, Tachibana M. H3K9 methyltransferase G9a and the related molecule GLP. Genes Dev. 2011;25(8):781-88
12. Mozzetta C, Pontis J, Fritsch L, et al. The histone H3 lysine 9 methyltransferases G9a and GLP regulate polycomb repressive complex 2-mediated gene silencing. Mol Cell. 2014;53(2):277-89
13. Sharma M, Sajikumar S. G9a/GLP complex acts as a bidirectional switch to regulate metabotropic glutamate receptor-dependent plasticity in hippocampal CA1 pyramidal neurons. Cereb Cortex. 2019;29(7):2932-46
14. Liang L, Zhao JY, Gu X et al. G9a inhibits CREB-triggered expression of mu opioid receptor in primary sensory neurons following peripheral nerve injury. Mol Pain. 2016;12:1744806916682242
15. Kim HT, Jeong SG, Cho GW. G9a inhibition promotes neuronal differentiation of human bone marrow mesenchymal stem cells through the transcriptional induction of RE-1 containing neuronal specific genes. Neurochem Int. 2016;96:77-83
16. Fiszbein A, Kornblihtt AR. Histone methylation, alternative splicing and neuronal differentiation. Neurogenesis (Austin). 2016;3(1):e1204844
17. Yang JJ, Xie MZ, Ju LS, et al. Enhanced histone lysine methyltransferase G9a might contribute to repeated sevoflurane exposure-induced apoptosis and cognitive impairment in the developing brain. Journal of Anesthesia and Perioperative Medicine. 2016;3(1):1-10
18. Jang JE, Eom JI, Jeung HK, et al. PERK/NRF2 and autophagy form a resistance mechanism against G9a inhibition in leukemia stem cells. J Exp Clin Cancer Res. 2020;39(1):66
19. Bellezza I, Giambanco I, Minelli A, Donato R. Nrf2-Keap1 signaling in oxidative and reductive stress. Biochim Biophys Acta Mol Cell Res. 2018;1865(5):721-33
20. Zeng J, Chen Y, Ding R, et al. Isoliquiritigenin alleviates early brain injury after experimental intracerebral hemorrhage via suppressing ROS- and/or NF-kappaB-mediated NLRP3 inflammasome activation by promoting Nrf2 antioxidant pathway. J Neuroinflammation. 2017;14(1):119
21. He J, Zhou D, Yan B. Eriocitrin alleviates oxidative stress and inflammatory response in cerebral ischemia reperfusion rats by regulating phosphorylation levels of Nrf2/NQO-1/HO-1/NF-kappaB p65 proteins. Ann Transl Med. 2020;8(12):757
22. Fu C, Zheng Y, Zhu J, et al. Lycopene exerts neuroprotective effects after hypoxic-ischemic brain injury in neonatal rats via the nuclear factor erythroid-2 related factor 2/nuclear factor-kappa-gene binding pathway. Front Pharmacol. 2020;11:585898
23. Xue H, Zhang YH, Gao QS, et al. Sevoflurane post-conditioning ameliorates neuronal deficits and axon demyelination after neonatal hypoxic ischemic brain injury: Role of microglia/macrophage. Cell Mol Neurobiol. 2020 [Online ahead of print]
24. Grinan-Ferre C, Marsal-Garcia L, Bellver-Sanchis A, et al. Pharmacological inhibition of G9a/GLP restores cognition and reduces oxidative stress, neuroinflammation and beta-Amyloid plaques in an early-onset Alzheimer's disease mouse model. Aging (Albany NY). 2019;11(23):11591-608
25. Xu Y, Tian Y, Tian Y, et al. Autophagy activation involved in hypoxic-ischemic brain injury induces cognitive and memory impairment in neonatal rats. J Neurochem. 2016;139(5):795-805
26. Wang J, Zheng H, Chen CL, et al. Sevoflurane at 1 MAC provides optimal myocardial protection during off-pump CABG. Scand Cardiovasc J. 2013;47(3):175-84
27. Shiraishi S, Cho S, Akiyama D, et al. Sevoflurane has postconditioning as well as preconditioning properties against hepatic warm ischemia-reperfusion injury in rats. J Anesth. 2019;33(3):390-98
28. Wang H, Lu S, Yu Q, et al. Sevoflurane preconditioning confers neuroprotection via anti-inflammatory effects. Front Biosci (Elite Ed). 2011;3:604-15
29. Pan MR, Hsu MC, Chen LT, Hung WC. G9a orchestrates PCL3 and KDM7A to promote histone H3K27 methylation. Sci Rep. 2015;5:18709
30. Wilson C, Giono LE, Rozes-Salvador V, et al. The histone methyltransferase G9a controls axon growth by targeting the RhoA signaling pathway. Cell Rep. 2020;31(6):107639
31. Schweizer S, Harms C, Lerch H, et al. Inhibition of histone methyltransferases SUV39H1 and G9a leads to neuroprotection in an in vitro model of cerebral ischemia. J Cereb Blood Flow Metab. 2015;35(10):1640-47
32. Subbanna S, Shivakumar M, Umapathy NS, et al. G9a-mediated histone methylation regulates ethanol-induced neurodegeneration in the neonatal mouse brain. Neurobiol Dis. 2013;54:475-85
33. Gupta R, Saha P, Sen T, Sen N. An augmentation in histone demethylation at lysine nine residues elicits vision impairment following traumatic brain injury. Free Radic Biol Med. 2019;134:630-43
34. Zhou C, Li H, Yao Y, Li L. Delayed remote ischemic preconditioning produces an additive cardioprotection to sevoflurane postconditioning through an enhanced heme oxygenase 1 level partly via nuclear factor erythroid 2-related factor 2 nuclear translocation. J Cardiovasc Pharmacol Ther. 2014;19(6):558-66
35. Li B, Sun J, Lv G, et al. Sevoflurane postconditioning attenuates cerebral ischemia-reperfusion injury via protein kinase B/nuclear factor-erythroid 2-related factor 2 pathway activation. Int J Dev Neurosci. 2014;38:79-86

Indexed in: [Current Contents/Clinical Medicine] [SCI Expanded] [ISI Alerting System] [ISI Journals Master List] [Index Medicus/MEDLINE] [EMBASE/Excerpta Medica] [Chemical Abstracts/CAS]